Increasing Perceived Safety in Motion Planning for Human-Drone Interaction

Sanne van Waveren
KTH Royal Institute of Technology
Stockholm, Sweden
sannevw@kth.se

Rasmus Rudling
KTH Royal Institute of Technology
Stockholm, Sweden
rrudling@kth.se

Iolanda Leite
KTH Royal Institute of Technology
Stockholm, Sweden
iolanda@kth.se

Patric Jensfelt
KTH Royal Institute of Technology
Stockholm, Sweden
patric@kth.se

Christian Pek
KTH Royal Institute of Technology
Stockholm, Sweden
pek2@kth.se

ABSTRACT

Safety is crucial for autonomous drones to operate close to humans. Besides avoiding unwanted or harmful contact, people should also perceive the drone as safe. Existing safe motion planning approaches for autonomous robots, such as drones, have primarily focused on ensuring physical safety, e.g., by imposing constraints on motion planners. However, studies indicate that ensuring physical safety does not necessarily lead to perceived safety. Prior work in Human-Drone Interaction (HDI) shows that factors such as the drone's speed and distance to the human are important for perceived safety. Building on these works, we propose a parameterized control barrier function (CBF) that constrains the drone's maximum deceleration and minimum distance to the human and update its parameters on people's ratings of perceived safety. We describe an implementation and evaluation of our approach. Results of a within-subject user study ($N = 15$) show that we can improve perceived safety of a drone by adjusting to people individually.

CCS CONCEPTS

• **Computer systems organization → Robotics**.

KEYWORDS

human-drone interaction, perceived safety, motion planning, control barrier functions

ACM Reference Format:
Sanne van Waveren, Rasmus Rudling, Iolanda Leite, Patric Jensfelt, and Christian Pek. 2023. Increasing Perceived Safety in Motion Planning for Human-Drone Interaction. In *Proceedings of the 2023 ACM/IEEE Int'l Conference on Human-Robot Interaction (HRI '23), March 13–16, 2023, Stockholm, Sweden.* ACM, New York, NY, USA, 10 pages. https://doi.org/10.1145/3568162.3576966

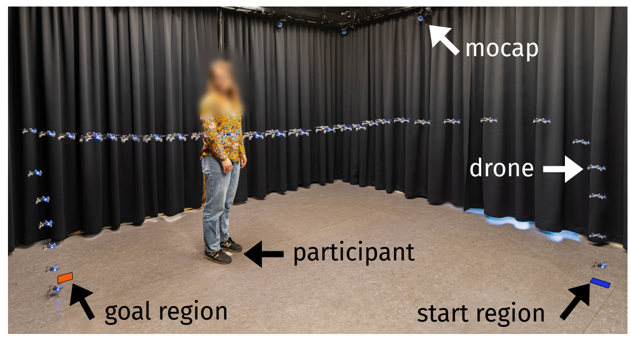

Figure 1: Overview of the drone study setup.

1 INTRODUCTION

Safety is crucial for autonomous drones that operate around humans [55], e.g., in delivery [39, 59], search-and-rescue [3, 44, 57], or firefighting tasks [4]. In such tasks, the drone must at all times avoid physical harm to objects and people in its environment, i.e., be physically safe. Ensuring safety is particularly difficult when the drone is required to operate close to humans (see Fig. 1), e.g., navigating around people. To date, safe motion planning for autonomous robots, such as drones, has primarily focused on ensuring physical safety [37]. For instance, by imposing constraints on motion planners [47], ensuring safety while tuning controller parameters [11], or using formal verification to ensure that the drone adheres to a given specification [8]. For instance, CBFs have become a popular tool to synthesize controllers with safety guarantees [17–19, 42, 60, 61]. However, studies indicate that ensuring physical safety does not necessarily lead to increased perceived safety [38, 54]. Besides being physically safe, drones should also be perceived as safe [37, 53].

Perceived safety is defined as how safe and comfortable a person feels during their interaction with a robot [9], which is affected by its appearance and behavior [14, 46]. When people perceive a robot as safe, they generally have higher trust in the robot, which increases acceptability [2] and decreases psychological stress in the long-term interaction [52]. Studies on perceived safety have studied the drone's appearance [69], interaction gestures [32], and found that the drone's distance, speed, and altitude are crucial factors [16, 53, 70]. These works in safe motion planning and HDI underline the need to explicitly consider both physical and perceived safety, when designing interactive robots. Yet, there does not exist work for motion planning of drones that investigates how to ensure physical safety while increasing perceived safety at the same time [53].

To address this gap, we propose a planning approach for drones using CBFs to ensure physical safety while allowing the drone to

HRI '23, March 13–16, 2023, Stockholm, Sweden

ACM ISBN 978-1-4503-9964-7/23/03.
https://doi.org/10.1145/3568162.3576966

adjust its perceived safety level. We formulate a CBF that allows us to adjust the drone's maximum deceleration (which serves as a proxy for its allowed velocity around the human) and the minimum distance to the human. We adjust these two parameters to people's feedback to obtain a personalized constraint function that we predict to result in drone behavior that is perceived as safe. We evaluate this personalized autonomous drone behavior in a controlled, yet realistic setting in a user study. The results advance our understanding of perceived safety in HDI and have implications for the design of safe motion planners for drones that improve perceived safety. We make the following contributions:

- An approach for improving perceived safety of drones in motion planning with physical safety guarantees by adjusting parameters (maximum deceleration and minimum distance to the person) of an personalized constraint function;
- A user study with a fully autonomous drone shows that adjusting these parameters to people individually results in higher levels of perceived safety.

While we showcase our approach with a search-based planner, it can be added as an additional check in most planning frameworks for a wide array of robot types.

2 RELATED WORK

Our planning approach combines concepts from motion planning, formal methods, and HRI. This section presents related works on perceived safety in HDI, increasing safety in robot motion planning and through formal verification.

2.1 Perceived safety in HDI

Factors such as the drone's speed, height, and relative distance to people affect perceived safety [16, 53]. Prior work found that people tend to generally feel comfortable with drone's that fly at moderate speeds of $0.5 - 0.7 m/s$ [21, 32, 70]. High robot speeds can cause people to feel unsafe, while slow robot motion can make people impatient [20]. Duncan and Murphy [21] explored how close people let a drone approach them and how the drone's altitude affects this stop distance. Results did not show that the drone's height affected the stop distance, which might have been confounded by a less realistic study scenario and the fact that participants were told the robot could not hurt them. Realism, complexity, and safety risks generally are factors that make it technically and ethically challenging to conduct user studies with fully autonomously flying drones [70]. Han and Bae [29] found that participants came closer to eye-level drones compared to overhead drones, but noted that participants were separated from the drone by an acrylic panel for safety. Hall [28] categorized distances that people keep to each other as the intimate ($0-0.45m$), personal ($0.45-1.2m$), social ($1.2-3.65m$), and public ($> 3.6m$) distance zones. HRI studies have shown that people tend to maintain similar interpersonal distance zones with robots as they do with people [1, 15, 31, 40, 46, 51, 56, 63, 65, 67, 70].

2.2 Increasing safety in motion planning

Motion planners should avoid states in which the robot cannot avoid collisions [10, 22], including collisions between robots and humans [27]. Some works have focused on improving human-robot handovers by placing constraints on motion planning [20, 43, 62]; for instance, to ensure that the robot is in a low inertia configuration and maintains a safe distance from the human [36]. In model predictive control approaches [30, 48], the robot is replanning its motion in regular intervals to account for changes in the environment. Combining this reactive scheme with predictions of the human can offer probabilistic guarantees on physical safety [41], e.g., a collision will not happen with 90% probability. An increasing body of work has shown that human-aware motion planners can increase perceived levels of safety. Lasota and Shah [38] showed that a human-aware motion planner for a collaborative robot improved team efficiency and people felt safer and more comfortable during the interaction. Other works have used constraints in motion planning to improve passenger comfort in autonomous transportation [33, 45]. While these motion planning approaches have shown to improve safety, they cannot provide formal safety guarantees, i.e., that the robot is physically safe at all times.

2.3 Ensuring safety through formal verification

Since computing unsafe states in which the robot cannot avoid collisions can be computationally complex, passively safe motion planners ensure that the robot is at least at standstill before a collision occurs [13]. Reachability analysis has become a popular technique to verify the safety of arbitrary motions. This technique computes the set of states that a system is able to reach over time considering all admissible trajectories. Safety is guaranteed when the robot's reachable set does not intersect with unsafe regions [7, 26, 35, 50, 58].

Control invariant sets have been used to ensure that the robot can always find a safe action from its current state [5, 12, 34]. However, computing these sets is usually difficult for arbitrary planners. CBFs are functions that generate constraint sets that are forward invariant, they can be used as a constraint in many motion planning frameworks [6]. Yet, over-approximations of worst-case scenarios and system abstractions can lead to overly conservative behavior. Some constraints might need to be relaxed to avoid overly conservative behavior that is perceived as safer than needed. Recently, Cosner et al. [19] used user feedback to approximate the constraint set of a CBF to avoid unsafe actions without being overly conservative in a safety-critical quadrupedal robot. Building on these approaches, we propose safe controller synthesis using CBFs that are tuned to optimize physical safety and perceived safety of a drone that flies close to people. Our approach is the first to increase perceived safety of an autonomous drone in motion planning by adjusting to people's individual feedback while also providing physical safety guarantees.

3 METHOD

This section describes our HDI model in Sec. 3.1, the CBF (Sec. 3.2) and its parameter calibration (Sec. 3.3), and how we integrate our CBFs into the motion planner (Sec. 3.4).

3.1 Human-drone interaction model

We consider a drone that operates in the proximity of a static human and model the HDI as a coupled system through relative distances. Here, $p_D \in \mathbb{R}^2$ and $p_H \in \mathbb{R}^2$ describe the drone's and human's positions in the horizontal plane, respectively, and $s = ||p_D - p_H||_2$ denotes the relative distance between the drone and the human.

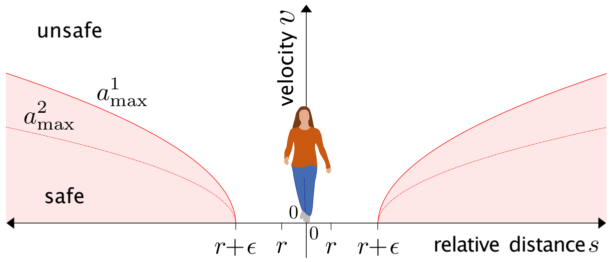

Figure 2: Illustration of our CBF in the $s - v$–plane where the human's position is at $s = 0$. Here, ϵ encodes the drone's minimum distance to the human and $a_{\max}$ constrains the drone's velocity in the human's proximity.

When the drone moves around the human with absolute velocity $v(t)$, the relative distance $s(t)$ changes. Since efficient onboard controllers enable the drone to track positions in 2D reasonably fast, we model the drone's motion towards the human as a double integrator system [25] with state x and control input u.

3.2 CBF synthesis for perceived safety

The drone should never collide with the human, i.e., it must always be able to stop in time. Moreover, for perceived safety, we adjust the drone's minimum allowed distance to the human and its allowed velocity in the human's proximity. Fig. 2 illustrates the safe set created by the CBF in the $s - v$–plane. We describe the human's occupied space by a circle with center p_H and radius $r \in \mathbb{R}_+$. Inspired by the recent research on CBFs for double integrator systems [17, 25, 49, 60, 72], we design a CBF $h(x)$ to ensure these two safety constraints:

$$h(x) = s(t) - \underbrace{(v(t)^2/2a_{\max})}_{①} - \underbrace{(r + \epsilon)}_{②} \geq 0, \quad (1)$$

where $\epsilon \in \mathbb{R}_{\geq 0}$ encodes the minimum distance to the human and $a_{\max} \in (0, u_{\max}]$ encodes the drone's deceleration, where $u_{\max}$ is the drone's maximum absolute deceleration. With this deceleration, we can compute the drone's stop distance and solve for the maximum allowed velocity as in [49]. This maximum allowed velocity is encoded in the term ① and enforces that the drone can still stop in time when flying straight towards the human by braking with $a_{\max}$ considering its double integrator dynamics (see Sec. 3.1). Hence, the drone's maximum allowed deceleration $a_{\max}$ serves as a proxy for its maximum allowed velocity. The term ② ensures that the drone stops minimally ϵ far away from the human. Eq. (1) is a valid CBF, since it ensures that the drone can always execute a full braking trajectory that satisfies the constraint. A full proof can be obtained by adding our two parameters to a CBF proof as in [25].

In general, our CBF enforces that the drone keeps a minimum safe distance from the human with respect to its velocity, ensuring that the drone can always stop in time. The parameter $a_{\max}$ shapes the maximum allowed velocity as parabolic arcs, since we consider a double integrator system: smaller values of $a_{\max}$ reduce the drone's velocity when coming closer to the human, as shown by $a_{\max,2} < a_{\max,1}$. Note that we obtain a least-restrictive CBF by setting the minimum distance to the human to the smallest allowed value ($\epsilon = \epsilon_{\min}$) and the allowed deceleration to the maximum value ($a_{\max} = u_{\max}$), and thus only considering physical safety.

3.3 Estimating parameters for perceived safety

We hypothesize that adjusting the parameter pair $(\epsilon, a_{\max})$ to people individually will improve perceived safety (Sec. 4.1). While more aggressive values, higher $a_{\max}$ and smaller ϵ might be perceived as too unsafe, more defensive parameter values might be perceived as overly safe. We aim to approximate the unknown perceived safety function $P : (\epsilon, a_{\max}) \mapsto \rho \in \mathcal{P}$ that maps a pair $(\epsilon, a_{\max})$ to its expected perceived safety value $\rho \in \mathcal{P}$, where $\mathcal{P}$ is a desired value range corresponding to the 7-points scale:

- -3 (too unsafe): if you feel like the drone flew too fast and uncomfortably close to you.
- 0 (safe): if you think the drone flew at an ideal distance from you with an ideal velocity.
- 3 (overly safe): if you feel like the drone flew too slow and unnecessarily far away from you.

Our goal is to find the value pair $(\epsilon^*, a^*_{\max})$ to synthesize a CBF that yields a perceived safety of zero $\rho = 0$. We propose a data-driven approach based on Gaussian Processes (GPs) [68] to find people's individual parameter pair $(\epsilon^*, a^*_{\max})$. GPs allow us to approximate an unknown function through samples of it. Our approach is similar to Bayesian Optimization [23], but deviates from the typical process in that we are trying to reduce the overall uncertainty in the function's approximation. Our intuition behind this is that the parameter pair that yields a safe score $\rho = 0$ is not necessarily unique. To discover the whole 0-level set, we chose our sampling strategy to reduce overall variance in our safety function approximation $\mathcal{P}$. We collect M samples of pairs $(\epsilon^i, a^i_{\max}), i \in \{1, M\}$, synthesize a CBF for each of them, and collect feedback on the perceived safety ρ^i through human experiments. Note that larger values of M gather more information on the unknown perceived safety function and lead to better approximations. Alg. 1 summarizes the steps to determine the optimal pair $(\epsilon^*, a^*_{\max})$ for a number of M desired samples as $(\epsilon^*, a^*_{\max}) = \text{argmin}_{\epsilon, a_{\max}} |P(\epsilon, a_{\max})|$, referred to as *personal* CBF h_P throughout the remainder of the paper.

3.4 Motion planning for perceived safety

Each chosen parameter pair $(\epsilon, a_{\max})$ creates a valid CBF that we can use as constraints in a motion planner. In general, the drone plans a trajectory $x^*_{k,k+H}$ from time step t_k to $t_{k+H}, H \in \mathbb{N}_{\geq k}$ that minimizes a given cost function J. We can formulate this motion planning as an optimization problem subject to constraints:

$$\begin{aligned} x^*_{k,k+H} = \underset{x,u}{\text{argmin}} & \sum_i J(x_{k+i+1}, u_{k+i}) \\ \text{subject to } & x_k = x_I, \\ & x_{k+i+1} = F(x_{k+i}, u_{k+i}), \\ & h(x_{k+i+1}) \geq 0, \\ & i \in \{0, H-1\}, \end{aligned} \quad (2)$$

where x_I is the drone's safe initial state and F is the state transition function. By definition, any pair $(\epsilon, a_{\max})$ ensures physical safety: the drone can always execute a full braking trajectory that does

Algorithm 1 Parameter estimation for perceived safety

Require: desired iterations M

$D \leftarrow \emptyset$

$P \leftarrow \text{initGP}()$

for $i \leftarrow 1, M$ **do**

  $(\epsilon^i, a^i_{\max}) \leftarrow \text{sampleFromGP}(P)$

  $\rho^i \leftarrow \text{evaluatePerceivedSafety}(\epsilon, a_{\max})$

  $D \leftarrow D \cup \{(\epsilon^i, a^i_{\max}, \rho^i)\}$

  $P \leftarrow \text{trainGP}(D)$

$(\epsilon^*, a^*_{\max}) \leftarrow \text{argmin}_{\epsilon, a_{\max}} |P(\epsilon, a_{\max})|$

not result in a collision with the human. This emergency maneuver can be precomputed and executed in safety-critical situations. The choice of $(\epsilon, a_{\max})$ influences the drone's maximum allowed velocity in the human's proximity as well as the minimum allowed distance to the human. Note that (2) is only one possible formulation. Our CBF constraint can also be added to other motion planning frameworks as outlined for CBFs in [6].

4 RESEARCH APPROACH

We evaluate our planning approach to increase perceived safety in motion planning for drones in a within-subjects study with an autonomous drone. We first describe our hypotheses (Sec. 4.1), experimental conditions (Sec. 4.2), and experimental setup (Sec. 4.3). Then, we describe the pre-study's and the main study's experimental procedure (Sec. 4.4) and participants (Sec. 4.5).

4.1 Hypotheses

Prior work suggests that ensuring a robot's physical safety does not necessarily lead to increased perceived safety [38, 54]. To ensure both task performance and perceived safety, we need to optimize both objectives in the motion planner. For instance, Fig. 3 illustrates a drone that needs to fly from *start* to *goal* with a human in between. We want the drone to be perceived as safe and keep appropriate speed and distance when flying close to the human. At the same time, we want it to reach its goal as quickly as possible and avoid a large detour or too slow speeds which might be perceived as overly safe and inefficient, leaving room for more task performance. While task performance can be measured and optimized for in the motion planning, we need to investigate how we can model perceived safety as part of the drone's task and whether we can increase it by adjusting to the individual. Further, we explore whether it is sufficient to calibrate perceived safety based on the ratings of a small set of people only without further adjustment to individual users, which would reduce load on the user. To fill the gaps in existing literature, we formulated the following hypotheses:

- **H1** A drone that adapts to people, either as a group or individually, will be perceived as safer than a drone that adapts according to predefined proxemics zones;
- **H2** A drone that adapts to people individually will be perceived as safer than a drone that aggregates feedback from an initial set of people but does not adjust to the individual.

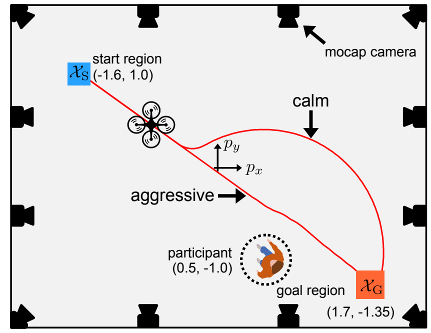

Figure 3: Experiment room overview with a participant in a designated area and the drone flying from start to goal region. We also plot our calm and aggressive baseline trajectories.

4.2 Conditions

To test our hypotheses, we conducted a within-subjects study to compare the perceived safety of the following constraint functions:

(1) *aggregated* CBF h_A: this CBF's parameters are adjusted to all three participants in our pre-study (see Sec. 4.4.1);
(2) *personal* CBF h_P: this CBF's parameters are determined for individual participants in our main study and do not consider the parameters obtained in the pre-study (see Sec. 4.4.2);
(3) *heuristic* h_E: a hand-crafted heuristic function that is inspired by Hall's proxemics zones (more details in Sec. 4.3.1).

4.3 Experimental Setup

4.3.1 Heuristic constraint function. We compare our CBF-based constraint functions with a hand-crafted heuristic h_E, inspired by the interpersonal distance zones as defined by Hall [28]. We keep the velocity constant in each zone and choose it based on our *aggregated* CBF h_A. In this way, we obtain a more conservative version of our aggregated CBF that aligns with the proxemics zones. The *heuristic* h_E is defined as $h_E(x) = v_{\max}(s) - v(t) \geq 0$, where the maximum velocity $v_{\max}(s)$ is computed as:

$$v_{\max}(s) := \begin{cases} 0 & \text{for } s \in [0.0m, 0.45m), \\ \sqrt{2(0.45 - \epsilon_A)a_{\max,A}} & \text{for } s \in [0.45m, 1.2m), \\ \sqrt{2(1.2 - \epsilon_A)a_{\max,A}} & \text{for } s \in [1.2m, 3.5m), \\ \sqrt{2(3.5 - \epsilon_A)a_{\max,A}} & \text{for } s \geq 3.5m, \end{cases} \tag{3}$$

where $\epsilon_A = 0.1$ and $a_{\max,A} = 0.52$ come from the *aggregated CBF* h_A (see Tab. 1).

4.3.2 Motion planner. In the study, the drone starts from the region $\mathcal{X}_S$ with center $(-1.6, 1.0)$ and flies to the goal region $\mathcal{X}_G$ with center at $(1.7, -1.35)$, see Fig. 3. We want the drone to take the shortest path from start to goal. We implement an A*-based motion planner to plan the drone's trajectory while adhering to the chosen constraint function (CBF or heuristic). The drone's motion consists of three different maneuvers: take-off, flying from start to goal region, and landing. During the take-off maneuver, the drone flies upwards to a height of $\ell_H - 0.5m$, where ℓ_H is the human's height in meters. Prior work found no difference in comfort for small drones that fly above or below head height [21], we chose the drone's altitude to be around chest level (see Fig. 4). During the

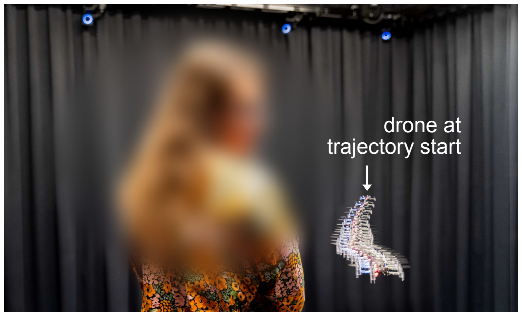

Figure 4: Participant experiencing the drone with the aggressive baseline trajectory, i.e., $\epsilon = \epsilon_{\min} = 0.1$ and $a_{\max} = 1$.

Figure 5: A Bitcraze Crazyflie drone that we used in our study.

landing maneuver, the drone lands in the goal region $\mathcal{X}_G$. We set the minimum and maximum absolute velocity of the drone during flight to $0.2 m/s$ and $1.5 m/s$, respectively.

4.3.3 Apparatus. We use a Bitcraze Crazyflie 2.1 drone with dimensions $92x92x29$mm (length x width x height) (Fig. 5), which can fly up to 7 minutes on one battery charge. We use an OptiTrack Motion Capture system with 12 cameras to track the drone.

4.4 Experimental Procedure

4.4.1 Pre-study. After participants gave their written consent, they read the study's instructions and provided their height, which was used to adjust the drone's altitude. Then, participants entered the study room and were instructed to stand in a dedicated spot marked on the floor, facing the drone which was placed in the start region, as illustrated in Fig. 3. Prior to the actual experiment, participants went through a calibration phase in which they witnessed two baseline trajectories (see also Fig. 3 and Fig. 4): one with the most calm parameter pair possible ($\epsilon_{\text{calm}} = 0.75, a_{\text{max,calm}} = 0.1$) and one demonstrating the most aggressive trajectory ($\epsilon_{\text{aggr}} = 0.1, a_{\text{max,aggr}} = 1$). This calibration was conducted to establish some notion of the extreme anchors of the 7-points scale range (-3 to 3) to rate trajectories' perceived safety. Two people saw the aggressive trajectory first and one person saw the calm trajectory first.

During each trial in the study, participants saw the drone lift off, fly from the start to the goal region, and land (see Fig. 1). In total, three participants completed 5 trials, resulting in $3x5 = 15$ trials across participants from which we compute the *aggregated* CBF h_A. Participants were instructed to stand still, but were allowed to move their head and eyes to follow the drone with their gaze. After each trial, they were asked to rate the question "*How did you perceive the most recent trajectory?*" via a smartphone mounted next to the participant on the 7-points, see Sec. 3.3. We updated the parameters in each trial according to Alg. 1 across the three participants, which means that only the first participant started their first trial with a random parameter configuration, all following trials used the updated CBF. The experiment took around 20 minutes and participants were compensated an equivalent of about 9USD.

The final parameters for the *aggregated* CBF h_A are listed in Table 1. Fig. 6 illustrates our approximated perceived safety function P from our pre-study, where we used a value range of $\mathcal{P} = [-3, 3]$, $M = 15$ samples, and radial-basis functions for the GP [68]. Optimal values $(\epsilon^*, a^*_{\max})$, i.e., $P(\epsilon^*, a^*_{\max}) = 0$, are usually not unique (see black lines in Fig. 6). In such cases, we choose a random pair on the corresponding level set, since all those pairs are estimated to have optimal perceived safety.

4.4.2 Main Study. The procedure is the same as our pre-study in Sec. 4.4.1, except for that after the calibration phase, the experiment now consisted of two phases: a personalization phase and a comparison phase. Since we are estimating perceived safety for one participant here instead of a group, we empirically chose to collect $M = 7$ samples of pairs $(\epsilon^i, a^i_{\max}), i \in \{1, M\}$ as this number of trials was feasible on one drone battery charge and took a reasonable duration for participants to perform a single activity. Participants first completed 7 trials to compute their *personalized CBF* h_P. After this phase, there was a brief pause where the drone's battery was changed and participants could take a break for a couple of minutes. Then in the comparison phase, each participant rated each of the three constraint functions in Sec. 4.2 twice, resulting in a total of six trials in randomized order to reduce order effects. An equal number of participants started with each constraint function first (i.e., in the first trial). Table 1 lists the average parameters across participants.

4.5 Participants

Pre-study. One female and two male participants of Swedish nationality took part in the pre-study ($N_{\text{pre}} = 3$). They were between 22-65 years of age ($\mu = 37.67, \sigma = 23.76$) with heights between

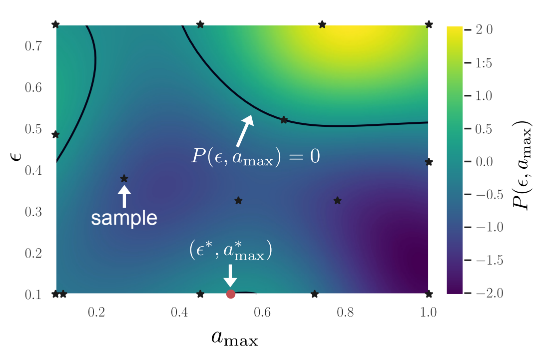

Figure 6: Resulting GP when training with the data from all participants in the pre-study.

Table 1: Obtained parameters for the CBFs.

CBF	ϵ^*	$a^*_{\max}$
Aggregated h_A	0.1	0.52
Personal h_P	$\mu = 0.42, \sigma = 0.27$	$\mu = 0.56, \sigma = 0.27$

1.60m-1.87m (μ = 1.72m, σ = 0.14m). All participants have previously seen a drone fly in person but never interacted with a drone. Two participants' completed a Bachelor's degree, and one participant completed a Master's degree. Two participants wore safety glasses, one participant wore their regular glasses.

Main study. Five female and ten male (N_{main} = 15) between 23 and 55 years of age (mean age μ = 28.67 and σ = 7.75) took part in the study. Their nationalities were Swedish (8), Chinese (2), Indian (2), German (2), and Italian (1). The mean height was μ = 1.75m (σ = 0.09m). Four participants wore their regular glasses, nine participants wore safety glasses provided by the experimenter, and for two participants the safety glasses were omitted by mistake. Two participants had never seen a drone fly before, three participants had seen a drone fly in videos, five participants had seen a drone fly in person before, and five participants controlled a real drone before. One participant took college courses but had no official degree, three participants had a Bachelor's degree, 10 participants had a Master's degree, and one participant had a Doctoral degree.

5 RESULTS

This section discusses the results of our user study. First, we evaluate perceived safety ratings from the two baseline trajectories participants saw in the calibration phase Sec. 5.1. Then, we discuss the comparison of perceived safety ratings between conditions in Sec. 5.2. Finally, Sec. 5.3 and Sec. 4.5 discuss our in-depth evaluation of the obtained personal CBFs and parameters. The code of our CBFs and experimental data are publicly available: github.com/Sannevw/hri2023-persafe.

5.1 Calibration results

To check that our calm and aggressive baseline trajectories were perceived as intended in the calibration phase, we evaluate people's perceived safety ratings from the pre-study and main study combined. As ratings for the two baseline trajectories were not normally distributed, we conducted a Wilcoxon signed rank test on the ratings. As can be seen in Fig. 7a, on average the calm trajectory was rated higher on perceived safety, leaning towards being more safe than needed (both studies combined: $\mu total$ = 1.78, σ_{total} = 1.31; pre-study: μ_{pre} = 1, σ_{pre} = 2; main study: μ_{main} = 1.93, σ_{main} = 1.16) than the aggressive trajectory which was perceived as less safe than needed (both studies combined: μ_{total} = −0.72, σ_{total} = 1.81; pre-study: μ_{pre} = −1.67, σ_{pre} = 2.31; main study: μ_{main} = −1.33, σ_{main} = 0.98), Z= 17.5, p<.005, η^2 = .703.

5.2 Perceived safety ratings

We conducted a repeated measures ANOVA to examine the effect of condition (constraint function) on perceived safety levels. The constraint function had a statistically significant effect on perceived

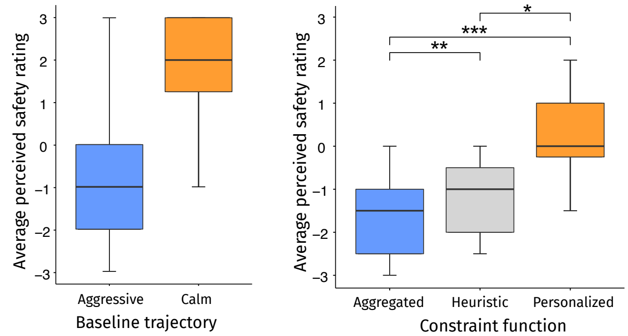

(a) (b)

Figure 7: Average perceived safety for (a) the two baseline trajectories computed for pre- and main study participants combined, and (b) the three constraint functions in the main study. Zero indicates *safe*. *p<.05, **p<.005, ***p<.001.

safety levels, $F(2, 28)$ = 16.37, p<.0001, η^2 = .445 (See Fig. 7b). Post hoc analysis with a Bonferroni adjustment revealed that the *personal* CBF h_P was perceived as safest (μ = 0.17, σ = 1.03), the *heuristic* function h_E was perceived as less safe than needed (μ = −1.17, σ = 0.79), but safer than the *aggregated* CBF h_A, which was rated the least safe (μ = −1.77, σ = 0.96). These results support **H2** that a drone that adapts to people individually (*personal* CBF h_P) lead to higher perceived safety ratings than a drone that adapts to a group of people (*aggregated* CBF h_A). Our results seemed to only partially support **H1**, as the drone that adapted to a group of people (*aggregated* CBF h_A) was perceived as less safe than a drone that adapts according to predefined proxemics zones (*heuristic* h_E).

5.3 Comparison of the personal CBFs

To better understand what drone parameters (velocity and relative distance) people preferred, we inspect the parameters of the personal CBFs we obtained for each of the N_{main} = 15 participants in more depth. The drone's trajectory for the *personal* CBF h_P had an average duration of μ = 11.71s (σ = 2.92) with an average maximum velocity of μ = 1.15m/s (σ = 0.22). Table 1 summarizes the average values for ϵ^* and $a^*_{\max}$ in the main study. In general, we observed that the optimal parameters have a larger standard deviation, confirming that perceived safety is subject to the individual. Fig. 8 illustrates the executed trajectories of all participants as well as our two baseline trajectories. Considering the minimum allowed distance to the human controlled by ϵ, we see that the participants tended to prefer values closer to the aggressive baseline. Fig. 9 shows the generated velocity constraints from the *personal* CBF h_P, the *aggregated* CBF h_A, the *heuristic* h_E, as well as our two baselines. On average, participants preferred a rather neutral velocity profile in between the aggressive and calm baselines.

Our results suggest that we can identify subgroups in our participants. We performed a cluster analysis using affinity propagation [24] which identifies points in our data that are most representative of the other participants. Fig. 10 illustrates our cluster analysis in which we found four clusters.

Two clusters with 2 participants prefer either a defensive velocity constraint with a more aggressive (i.e., smaller) minimum allowed

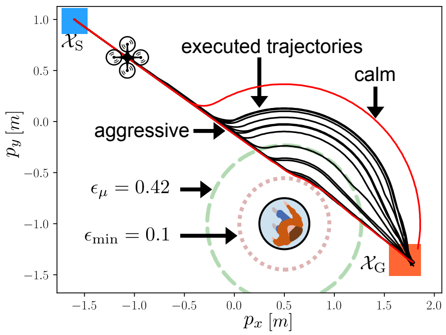

Figure 8: Executed trajectories that have been planned with the personalized CBFs for all participants as well as our calm and aggressive baseline trajectories. We also plot the minimally allowed distance to the human for $\epsilon = 0.1$ and the average $\epsilon_\mu = 0.42$ while considering the drone's dimensions.

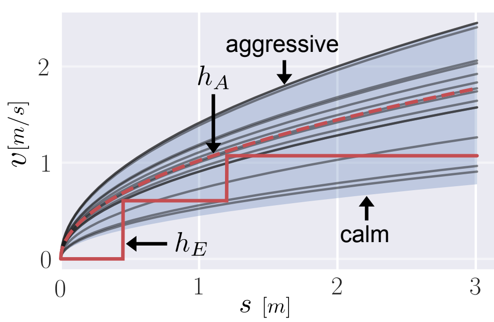

Figure 9: Computed velocity constraints for personalized CBFs of all participants, the *aggregated* CBF h_A, and for the *heuristic* function h_E. For easier comparison, we plot the CBFs with $\epsilon = 0$. The shaded region contains all velocity profiles between our calm and aggressive baselines.

distance ($a_{\max} < 0.2$, $\epsilon < 0.15$, see ❶ in Fig. 10) or a more aggressive velocity constraint but a more defensive (i.e., larger) minimum allowed distance ($a_{\max} > 0.9$, $\epsilon > 0.6$, see ❷ in Fig. 10). The second largest cluster with 4 participants (❸ in Fig. 10) prefers a more moderate-to-aggressive velocity constraint ($a_{\max} > 0.4$) and a small minimum allowed distance ($\epsilon < 0.15$). The biggest cluster with 7 participants (❹ in Fig. 10) prefers a moderate velocity constraint ($0.25 \leq a_{\max} \leq 0.7$) and a larger distance to the drone ($\epsilon > 0.35$).

5.4 Parameter analysis for perceived safety

To further analyze the effect of our CBF parameters on perceived safety, we trained a GP with the data of all participants of our main study. In this way, we approximate the perceived safety function P with 105 datapoints. Fig. 11 illustrates the resulting GP. In general, we observe that a larger minimum distance ϵ is perceived as more safe than needed with rating of $\rho > 1.5$. In contrast, a fast moving drone close to the participant is perceived as less safe than needed. When analyzing the value pairs for which the function estimates a safe score, $P(\epsilon, a_{\max}) = 0$, we notice two general trends. We computed Spearman's rank correlation to assess the relationship

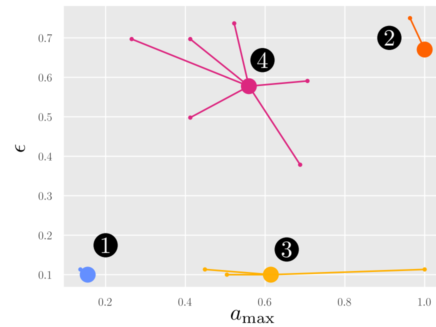

Figure 10: Our cluster analysis with affinity propagation [24] indicates the presence of four clusters. Large points are the representative points for each cluster.

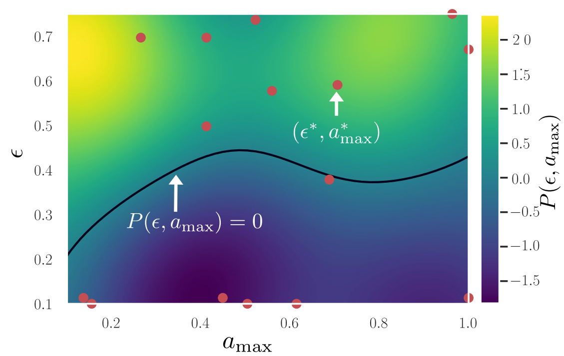

Figure 11: Resulting GP trained on data of all main study participants showing the trend that larger distances are perceived as overly safe while a fast-moving drone close to participants is perceived as less safe than needed. We also overlay the chosen optimal parameters for each participant individually (red dots). Note that those values are chosen from different GPs which are trained on that person's data only and therefore deviate from the optimal values for all participants (black line).

between all parameter pairs. They were found to be moderately positively correlated, $r(74) = .56$, $p<.0001$, which indicates that as $a_{\max}$ increases, ϵ increases too but not in a linear fashion. Manual inspection of Fig. 11 revealed a potential strong linear relationship between the two parameters for $0.1 \leq \epsilon \leq 0.4$ and $0.1 \leq a_{\max} \leq 0.4$ at $P = 0$. A Pearson correlation coefficient was computed to assess the linear relationship between $a_{\max}$ and ϵ. There was a strong positive correlation between the two parameters, $r(28) = .99$, $p<.0001$, suggesting that as the maximum allowed velocity increases in this range, minimum allowed distance increases as well.

6 DISCUSSION

To date, safe motion planning has primarily focused on physical safety. Some recent works have shown the success of increasing perceived safety levels in motion planning, e.g., for handovers [20, 43, 62]. Extending these works, we introduced a new planning approach for drones which provides safety guarantees and optimizes for task performance and perceived safety using a personalized control barrier function (CBF). We described how we can find personal parameter pairs that encode people's preferred drone's maximum allowed velocity ($a_{\max}$) and minimum allowed distance to the person (ϵ) and evaluated whether these *personal* CBFs improve perceived safety of the drone.

6.1 Perceived safety through personalization

The results support **H2** as the perceived safety was significantly higher for the *personal* CBF h_P than an *aggregated* CBF h_A. This outcome is a strong indication that human-drone interaction can significantly benefit from motion planners that are adjusted to the individual, extending prior work that showed human-aware motion planning is beneficial [20, 33, 43, 45, 62].

To reduce user load, we wanted to see if we could achieve perceived safety by obtaining an initial parameter pair by aggregating data from a small set of people ($M_{pre} = 3$). While our small sample size does not enable us to strong conclusions and we leave this to future work, our results seem to only partially support **H1** as the *aggregated* CBF h_A was perceived as less safe than the *heuristic* h_E (Fig. 7b). Since our results suggest that participants in our main study could be clustered as subgroups, we speculate that the small number of participants in the pre-study might have affected our results, and it might require more data points from more people to approximate a more representative parameter pair ($\epsilon, a_{\max}$) for the *aggregated* CBF h_A. Another possible explanation might be that the *heuristic* h_E function essentially was a more conservative version of the *aggregated* CBF h_A (see Sec. 4.3.1). Contrary to the *aggregated* CBF h_A, the *heuristic* h_E has a constant maximum velocity between personal zones instead of a constantly changing maximum velocity (Fig. 9). This is in line with prior work that identified predictability as a key factor of perceived safety [52, 64].

6.2 Choosing drone parameters

We also approximated a perceived safety function using all participants in the main study. Analysis of the resulting GP, seems to suggest that the minimum distance linearly increases with the maximum allowed velocity of the drone for small distances and velocities, but for larger velocities ($a_{\max} > 0.4$) the distance does no longer increase linearly. To choose suitable parameters, Fig. 11 indicates that drones are allowed to come relatively close to people ($\epsilon \in [0.2, 0.5]$) when their allowed maximum velocity is low ($a_{\max} \in [0.2, 0.4]$). When the minimum distance to the human is around $0.5m$, people may accept that the drone flies with larger maximum velocities ($a_{\max} \in [0.5, 1.0]$). Additionally, our analysis revealed multiple subgroups in our data that can be roughly categorized into aggressive, neutral, and defensive parameter sets (see Fig. 10). This result suggest that drones could be equipped with different user profiles and users can choose the one that they prefer.

6.3 Limitations and Future Work

We performed the parameter estimation and planning in separate steps. In the future, the drone could actively query people on various trajectories that provide the most information gain for the GP. For comparison, we currently chose the maximum allowed velocity and minimum allowed distance for the heuristic to reflect the *aggregated* CBF h_A, which was obtained from a small number of participants. Future research needs to investigate if the results would hold when we aggregate data for a larger group of people and test the heuristic with a larger range of parameter values. Additionally, alternative ways to aggregate data must be investigated, e.g., finding similarities in individual GPs instead of updating one GP over multiple people. As our current sample size does not enable us to draw conclusions, future work could further investigate subgroups by validating our approach in a study with a larger sample size. Designing drone profiles from these subgroups is an interesting research direction when users want to quickly setup their drone or the drone is not able to collect people's feedback.

In this work, the drone flew around one static human who was observing the drone. Arguably, the human might be conducting other tasks and moving around while sharing space with the drone, it would be interesting to study perceived safety when the human is occupied with a secondary task and how to add a prediction term of human motion to our CBFs. If a drone has to adjust to a group, we need to further investigate if there exists a single parameter pair that is perceived as safe by everyone ($\rho > 0$) or if the drone should switch between different user profiles. The drone's size and appearance could affect the interaction [71], we looked at perceived safety in a short time exposure setting with a small drone. Over time, people could start perceiving a robot that acts aggressively but never causes accidents as safe. Overtrust describes the situation in which people might not fully understand the risks associated with the robot's behavior [66]. Future work needs to investigate how perceived safety can be modeled in long-term interactions. Communicating intent could mitigate this [32], how interaction modes could be integrated into our approach is left to future work.

7 CONCLUSIONS

Prior work has shown that human-aware motion planning can improve perceived safety. Extending these works, we proposed a motion planning approach for drones that ensures physical safety in the proximity of people through control barrier functions (CBFs) while at the same time optimizing for perceived safety. We designed a CBF which encodes the drone's maximum allowed deceleration (which serves as a proxy for its maximum allowed velocity) and its minimum allowed distance to people. By estimating the optimal parameters for each participant using Gaussian Processes, the drone can adjust its behavior to the individual. Our results demonstrate that adjusting these parameters to the individual leads to significantly higher perceived safety when interacting with a fully autonomous drone. Further, our data revealed interesting clusters that could be explored in future work. These findings advance our understanding of perceived safety in HRI and have implications for the design of safe drone behavior.

8 ACKNOWLEDGMENTS

This work was partially supported by the Wallenberg AI, Autonomous Systems and Software Program funded by the Knut and Alice Wallenberg Foundation and by the Vinnova Competence Center for Trustworthy Edge Computing Systems and Applications at KTH.

REFERENCES

[1] Urja Acharya, Alisha Bevins, and Brittany A Duncan. 2017. Investigation of human-robot comfort with a small unmanned aerial vehicle compared to a ground robot. In *Proc. of the IEEE/RSJ Int. Conf. on Intelligent Robots and Systems*. IEEE, 2758–2765.

[2] Neziha Akalin, Annica Kristoffersson, and Amy Loutfi. 2022. Do you feel safe with your robot? Factors influencing perceived safety in human-robot interaction based on subjective and objective measures. *Int. Journal of Human-Computer Studies* 158 (2022), 102744.

[3] Antonio Albanese, Vincenzo Sciancalepore, and Xavier Costa-Pérez. 2021. SARDO: An automated search-and-rescue drone-based solution for victims localization. *IEEE Transactions on Mobile Computing* 21, 9 (2021), 3312–3325.

[4] Omri Alon, Sharon Rabinovich, Chana Fyodorov, and Jessica R Cauchard. 2021. Drones in Firefighting: A User-Centered Design Perspective. In *Proc. of the Int. Conf. on Mobile Human-Computer Interaction*. ACM, 1–11.

[5] Daniel Althoff, Matthias Althoff, and Sebastian Scherer. 2015. Online safety verification of trajectories for unmanned flight with offline computed robust invariant sets. In *Proc. of the IEEE/RSJ Int. Conf. on Intelligent Robots and Systems*. IEEE, 3470–3477.

[6] Aaron D Ames, Samuel Coogan, Magnus Egerstedt, Gennaro Notomista, Koushil Sreenath, and Paulo Tabuada. 2019. Control barrier functions: Theory and applications. In *Proc. of the European control conference (ECC)*. IEEE, 3420–3431.

[7] Somil Bansal, Andrea Bajcsy, Ellis Ratner, Anca D Dragan, and Claire J Tomlin. 2020. A hamilton-jacobi reachability-based framework for predicting and analyzing human motion for safe planning. In *Proc. of the IEEE Int. Conf. on Robotics and Automation*. IEEE, 7149–7155.

[8] Fernando S Barbosa, Jesper Karlsson, Pouria Tajvar, and Jana Tumova. 2021. Formal Methods for Robot Motion Planning with Time and Space Constraints. In *Int. Conf. on Formal Modeling and Analysis of Timed Systems*. Springer, 1–14.

[9] Christoph Bartneck, Dana Kulić, Elizabeth Croft, and Susana Zoghbi. 2009. Measurement instruments for the anthropomorphism, animacy, likeability, perceived intelligence, and perceived safety of robots. *Int. Journal of Social Robotics* 1, 1 (2009), 71–81.

[10] Antoine Bautin, Luis Martinez-Gomez, and Thierry Fraichard. 2010. Inevitable collision states: a probabilistic perspective. In *Proc. of the IEEE Int. Conf. on robotics and automation*. IEEE, 4022–4027.

[11] Felix Berkenkamp, Angela P Schoellig, and Andreas Krause. 2016. Safe controller optimization for quadrotors with Gaussian processes. In *Proc. of the IEEE Int. Conf. on Robotics and Automation*. IEEE, 491–496.

[12] Franco Blanchini. 1999. Set invariance in control. *Automatica* 35, 11 (1999), 1747–1767.

[13] Sara Bouraine, Thierry Fraichard, and Ouahiba Azouaoui. 2016. Real-time safe path planning for robot navigation in unknown dynamic environments. In *CSA 2016-2nd Conference on Computing Systems and Applications*. CSA, 1–10.

[14] John Travis Butler and Arvin Agah. 2001. Psychological effects of behavior patterns of a mobile personal robot. *Autonomous Robots* 10, 2 (2001), 185–202.

[15] Jessica R Cauchard, Jane L E, Kevin Y Zhai, and James A Landay. 2015. Drone & me: an exploration into natural human-drone interaction. In *Proc. of the ACM Int. joint Conf. on pervasive and ubiquitous computing*. ACM, 361–365.

[16] Victoria Chang, Pramod Chundury, and Marshini Chetty. 2017. Spiders in the sky: User perceptions of drones, privacy, and security. In *Proc. of the CHI conference on human factors in computing systems*. ACM, 6765–6776.

[17] Yuxiao Chen, Mrdjan Jankovic, Mario Santillo, and Aaron D Ames. 2021. Backup control barrier functions: Formulation and comparative study. In *Proc. of the IEEE Conference on Decision and Control*. IEEE, 6835–6841.

[18] Wenceslao Shaw Cortez, Christos K Verginis, and Dimos V Dimarogonas. 2021. Safe, passive control for mechanical systems with application to physical human-robot interactions. In *Proc. of the IEEE Int. Conf. on Robotics and Automation*. IEEE, 3836–3842.

[19] Ryan Cosner, Maegan Tucker, Andrew Taylor, Kejun Li, Tamas Molnar, Wyatt Ubelacker, Anil Alan, Gábor Orosz, Yisong Yue, and Aaron Ames. 2022. Safety-Aware Preference-Based Learning for Safety-Critical Control. In *Learning for Dynamics and Control Conference*. PMLR, 1020–1033.

[20] Frédéric Dehais, Emrah Akin Sisbot, Rachid Alami, and Mickaël Causse. 2011. Physiological and subjective evaluation of a human–robot object hand-over task. *Applied ergonomics* 42, 6 (2011), 785–791.

[21] Brittany A Duncan and Robin R Murphy. 2013. Comfortable approach distance with small unmanned aerial vehicles. In *Proc. of IEEE RO-MAN*. IEEE, 786–792.

[22] Thierry Fraichard and Hajime Asama. 2004. Inevitable collision states—a step towards safer robots? *Advanced Robotics* 18, 10 (2004), 1001–1024.

[23] Peter I Frazier. 2018. Bayesian optimization. In *Recent advances in optimization and modeling of contemporary problems*. Informs, 255–278.

[24] Brendan J Frey and Delbert Dueck. 2007. Clustering by passing messages between data points. *Science* 315, 5814 (2007), 972–976.

[25] Azad Ghaffari, Imoleayo Abel, Daniel Ricketts, Sorin Lerner, and Miroslav Krstić. 2018. Safety verification using barrier certificates with application to double integrator with input saturation and zero-order hold. In *Proc. of the American Control Conference*. IEEE, 4664–4669.

[26] Jeremy H Gillula, Gabriel M Hoffmann, Haomiao Huang, Michael P Vitus, and Claire J Tomlin. 2011. Applications of hybrid reachability analysis to robotic aerial vehicles. *The Int. Journal of Robotics Research* 30, 3 (2011), 335–354.

[27] Sami Haddadin, Alin Albu-Schaffer, Alessandro De Luca, and Gerd Hirzinger. 2008. Collision detection and reaction: A contribution to safe physical human-robot interaction. In *Proc. of the IEEE/RSJ Int. Conf. on Intelligent Robots and Systems*. IEEE, 3356–3363.

[28] Edward T Hall. 1963. A system for the notation of proxemic behavior. *American anthropologist* 65, 5 (1963), 1003–1026.

[29] Jeonghye Han and Ilhan Bae. 2018. Social Proxemics of Human-Drone Interaction: Flying Altitude and Size. In *Companion of the 2018 ACM/IEEE Int. Conf. on Human-Robot Interaction*. IEEE, 376–376.

[30] Kevin Haninger, Christian Hegeler, and Luka Peternel. 2022. Model predictive control with Gaussian processes for flexible multi-modal physical human robot interaction. In *Proc. of the Int. Conf. on Robotics and Automation*. IEEE, 6948–6955.

[31] Helge Hüttenrauch, Kerstin Severinson Eklundh, Anders Green, and Elin A Topp. 2006. Investigating spatial relationships in human-robot interaction. In *Proc. IEEE/RSJ Int. Conf. on Intelligent Robots and Systems*. IEEE, 5052–5059.

[32] Walther Jensen, Simon Hansen, and Hendrik Knoche. 2018. Knowing you, seeing me: Investigating user preferences in drone-human acknowledgement. In *Proc. of the 2018 CHI Conference on Human Factors in Computing Systems*. ACM, 1–12.

[33] Jesper Karlsson, Sanne van Waveren, Christian Pek, Ilaria Torre, Iolanda Leite, and Jana Tumova. 2021. Encoding human driving styles in motion planning for autonomous vehicles. In *Proc. of the IEEE Int. Conf. on Robotics and Automation*. IEEE, 1050–1056.

[34] Melanie Kimmel and Sandra Hirche. 2017. Invariance control for safe human–robot interaction in dynamic environments. *IEEE Transactions on Robotics* 33, 6 (2017), 1327–1342.

[35] Shreyas Kousik, Patrick Holmes, and Ram Vasudevan. 2019. Safe, aggressive quadrotor flight via reachability-based trajectory design. In *Dynamic Systems and Control Conference*, Vol. 59162. American Society of Mechanical Engineers, V003T19A010.

[36] Dana Kulić and Elizabeth A Croft. 2005. Safe planning for human-robot interaction. *Journal of Robotic Systems* 22, 7 (2005), 383–396.

[37] Przemyslaw A Lasota, Terrence Fong, Julie A Shah, et al. 2017. A survey of methods for safe human-robot interaction. *Foundations and Trends® in Robotics* 5, 4 (2017), 261–349.

[38] Przemyslaw A Lasota and Julie A Shah. 2015. Analyzing the effects of human-aware motion planning on close-proximity human–robot collaboration. *Human factors* 57, 1 (2015), 21–33.

[39] Jangwon Lee, Haodan Tan, David Crandall, and Selma Šabanović. 2018. Forecasting hand gestures for human-drone interaction. In *Companion of the 2018 ACM/IEEE Int. Conf. on Human-Robot Interaction*. ACM/IEEE, 167–168.

[40] Rui Li, Marc van Almkerk, Sanne van Waveren, Elizabeth Carter, and Iolanda Leite. 2019. Comparing human-robot proxemics between virtual reality and the real world. In *Proc. of the ACM/IEEE Int. Conf. on human-robot interaction*. IEEE, 431–439.

[41] Shen Li, Nadia Figueroa, Ankit J Shah, and Julie A Shah. 2021. Provably Safe and Efficient Motion Planning with Uncertain Human Dynamics. In *Robotics: Science and Systems*. RSS, 1–18.

[42] Lars Lindemann and Dimos V Dimarogonas. 2020. Barrier function based collaborative control of multiple robots under signal temporal logic tasks. *IEEE Transactions on Control of Network Systems* 7, 4 (2020), 1916–1928.

[43] Jim Mainprice, E Akin Sisbot, Léonard Jaillet, Juan Cortés, Rachid Alami, and Thierry Siméon. 2011. Planning human-aware motions using a sampling-based costmap planner. In *Proc. of the IEEE Int. Conf. on Robotics and Automation*. IEEE, 5012–5017.

[44] Balmukund Mishra, Deepak Garg, Pratik Narang, and Vipul Mishra. 2020. Drone-surveillance for search and rescue in natural disaster. *Computer Communications* 156 (2020), 1–10.

[45] Yoichi Morales, Atsushi Watanabe, Florent Ferreri, Jani Even, Tetsushi Ikeda, Kazuhiro Shinozawa, Takahiro Miyashita, and Norihiro Hagita. 2015. Including human factors for planning comfortable paths. In *Proc. of the IEEE Int. Conf. on Robotics and Automation*. IEEE, 6153–6159.

[46] Jonathan Mumm and Bilge Mutlu. 2011. Human-robot proxemics: physical and psychological distancing in human-robot interaction. In *Proc. of the Int. Conf. on Human-robot interaction*. IEEE, 331–338.

[47] Tobias Nägeli, Lukas Meier, Alexander Domahidi, Javier Alonso-Mora, and Otmar Hilliges. 2017. Real-time planning for automated multi-view drone cinematography. *ACM Transactions on Graphics (TOG)* 36, 4 (2017), 1–10.

[48] Artemiy Oleinikov, Sanzhar Kusdavletov, Almas Shintemirov, and Matteo Rubagotti. 2021. Safety-aware nonlinear model predictive control for physical human-robot interaction. *IEEE Robotics and Automation Letters* 6, 3 (2021), 5665–5672.

[49] Christian Pek and Matthias Althoff. 2018. Efficient computation of invariably safe states for motion planning of self-driving vehicles. In *Proc. of the IEEE/RSJ Int. Conf. on Intelligent Robots and Systems*. IEEE, 3523–3530.

[50] Christian Pek, Stefanie Manzinger, Markus Koschi, and Matthias Althoff. 2020. Using online verification to prevent autonomous vehicles from causing accidents. *Nature Machine Intelligence* 2, 9 (2020), 518–528.
[51] Christopher Peters, Fangkai Yang, Himangshu Saikia, Chengjie Li, and Gabriel Skantze. 2018. Towards the use of mixed reality for hri design via virtual robots. In *1st International Workshop on Virtual, Augmented, and Mixed Reality for HRI (VAM-HRI), Cambridge, UK, March 23, 2020*. ACM, 1–4.
[52] Martina Raue, Bernhard Streicher, and Eva Lermer. 2019. *Perceived safety: A multidisciplinary perspective*. Springer.
[53] Matteo Rubagotti, Inara Tusseyeva, Sara Baltabayeva, Danna Summers, and Anara Sandygulova. 2022. Perceived safety in physical human–robot interaction—A survey. *Robotics and Autonomous Systems* 151 (2022), 104047.
[54] Maha Salem and Kerstin Dautenhahn. 2015. Evaluating trust and safety in HRI: Practical issues and ethical challenges. *Emerging Policy and Ethics of Human-Robot Interaction* (2015), 1–3.
[55] Pericle Salvini, Diego Paez-Granados, and Aude Billard. 2022. Safety Concerns Emerging from Robots Navigating in Crowded Pedestrian Areas. *Int. Journal of Social Robotics* 14, 2 (2022), 441–462.
[56] Aziez Sardar, Michiel Joosse, Astrid Weiss, and Vanessa Evers. 2012. Don't stand so close to me: users' attitudinal and behavioral responses to personal space invasion by robots. In *Proc. of the .ACM/IEEE Int. Conf. on Human-Robot Interaction*. IEEE, 229–230.
[57] David C Schedl, Indrajit Kurmi, and Oliver Bimber. 2021. An autonomous drone for search and rescue in forests using airborne optical sectioning. *Science Robotics* 6, 55 (2021), eabg1188.
[58] Sven R Schepp, Jakob Thumm, Stefan B Liu, and Matthias Althoff. 2022. SARA: A tool for safe human-robot coexistence and collaboration through reachability analysis. In *Proc. of the Int. Conf. on Robotics and Automation*. IEEE, 4312–4317.
[59] Judy E Scott and Carlton H Scott. 2019. Models for drone delivery of medications and other healthcare items. In *Unmanned aerial vehicles: Breakthroughs in research and practice*. IGI Global, 376–392.
[60] Andrew Singletary, Karl Klingebiel, Joseph Bourne, Andrew Browning, Phil Tokumaru, and Aaron Ames. 2021. Comparative analysis of control barrier functions and artificial potential fields for obstacle avoidance. In *Proc. of the IEEE/RSJ Int. Conf. on Intelligent Robots and Systems*. IEEE, 8129–8136.
[61] Andrew Singletary, Aiden Swann, Yuxiao Chen, and Aaron D Ames. 2022. Onboard safety guarantees for racing drones: High-speed geofencing with control barrier functions. *IEEE Robotics and Automation Letters* 7, 2 (2022), 2897–2904.
[62] Emrah Akin Sisbot and Rachid Alami. 2012. A human-aware manipulation planner. *IEEE Transactions on Robotics* 28, 5 (2012), 1045–1057.
[63] Leila Takayama and Caroline Pantofaru. 2009. Influences on proxemic behaviors in human-robot interaction. In *Proc. of the IEEE/RSJ Int. Conf. on Intelligent Robots and Systems*. IEEE, 5495–5502.
[64] Haodan Tan, Jangwon Lee, and Gege Gao. 2018. Human-drone interaction: Drone delivery & services for social events. In *Proc. of the ACM Conf. Companion Publication on Designing Interactive Systems*. ACM, 183–187.
[65] Tim van Oosterhout and Arnoud Visser. 2008. A visual method for robot proxemics measurements. In *Proceedings of Metrics for Human-Robot Interaction: A Workshop at the Third ACM/IEEE International Conference on Human-Robot Interaction (HRI 2008). Citeseer*. IEEE, 61–68.
[66] Alan R Wagner, Jason Borenstein, and Ayanna Howard. 2018. Overtrust in the robotic age. *Commun. ACM* 61, 9 (2018), 22–24.
[67] Michael L Walters, Kerstin Dautenhahn, René Te Boekhorst, Kheng Lee Koay, Christina Kaouri, Sarah Woods, Chrystopher Nehaniv, David Lee, and Iain Werry. 2005. The influence of subjects' personality traits on personal spatial zones in a human-robot interaction experiment. In *ROMAN 2005. IEEE Int. Workshop on Robot and Human Interactive Communication*. IEEE, 347–352.
[68] Christopher KI Williams and Carl Edward Rasmussen. 2006. *Gaussian processes for machine learning*. MIT press Cambridge, MA.
[69] Anna Wojciechowska, Jeremy Frey, Esther Mandelblum, Yair Amichai-Hamburger, and Jessica R Cauchard. 2019. Designing drones: Factors and characteristics influencing the perception of flying robots. *Proc. of the ACM on Interactive, Mobile, Wearable and Ubiquitous Technologies* 3, 3 (2019), 1–19.
[70] Anna Wojciechowska, Jeremy Frey, Sarit Sass, Roy Shafir, and Jessica R Cauchard. 2019. Collocated human-drone interaction: Methodology and approach strategy. In *Proc. of the ACM/IEEE Int. Conf. on Human-Robot Interaction*. IEEE, 172–181.
[71] Alexander Yeh, Photchara Ratsamee, Kiyoshi Kiyokawa, Yuki Uranishi, Tomohiro Mashita, Haruo Takemura, Morten Fjeld, and Mohammad Obaid. 2017. Exploring proxemics for human-drone interaction. In *Proc. of the Int. Conf. on human agent interaction*. IEEE, 81–88.
[72] Jun Zeng, Bike Zhang, and Koushil Sreenath. 2021. Safety-critical model predictive control with discrete-time control barrier function. In *Proc. of the American Control Conference*. IEEE, 3882–3889.